J. Astrophys. Astr. (2019) 40:35
https://doi.org/10.1007/s12036-019-9603-4

Tracing the outer disk of NGC 300: An ultraviolet view

CHAYAN MONDAL[1,2,*], ANNAPURNI SUBRAMANIAM[1] and KOSHY GEORGE[3]

[1]Indian Institute of Astrophysics, 2nd Block, Koramangala, Bengaluru 560 034, India.
[2]Pondicherry University, R.V. Nagar, Kalapet 605 014, India.
[3]Department of Physics, Christ University, Bengaluru, India.
*Corresponding author. E-mail: chayan@iiap.res.in

MS received 12 March 2019; accepted 11 July 2019; published online 19 August 2019

Abstract. We present an ultra-violet (UV) study of the galaxy NGC 300 using GALEX far-UV (FUV) and near-UV (NUV) observations. We studied the nature of UV emission in the galaxy and correlated it with optical, H I and mid-infrared (3.6 μm) wavelengths. Our study identified extended features in the outer disk, with the UV disk extending up to a radius of 12 kpc ($>2R_{25}$). We estimated the FUV and NUV disk scale-length as 3.05 $\pm$ 0.27 kpc and 2.66 $\pm$ 0.20 kpc respectively. The scale-length in FUV is 2.3 times larger than that at 3.6 μm, and we also find the disk to gradually become flatter from longer to shorter wavelengths. We performed a statistical source subtraction to eliminate the background contaminants and identified 261 unresolved UV sources between the radii 5.3 kpc and 10 kpc ($1 \sim 2R_{25}$). The identified UV sources show an age range between 1–300 Myr with a peak at 25 Myr and a mass range between $10^3 M_\odot$ to $10^6 M_\odot$, estimated using Starburst99 models. The north-eastern spiral arm is found to be populated by young low mass sources suggesting that the star formation in this spiral arm is a recent phenomenon. The UV emission beyond the R_{25} radius has contribution from these low mass sources and is extended up to $\sim 2R_{25}$ radius. We conclude that NGC 300 has an extended UV disk, mainly populated by young low mass sources. The star formation rate is measured to be $\sim$0.46 $M_\odot$/yr which is comparable to its near optical twin M33.

Keywords. Individual galaxies—spiral galaxies—star formation—XUV disk.

1. Introduction

Evolution of galaxies over a time scale is dictated by its star formation. The star formation in the outer disks of galaxies has attracted a lot of attention recently, where these studies are centered around the nearby galaxies (Thilker *et al.* 2005a, b, 2007; Gil de Paz *et al.* 2005). The outer parts of the galaxies where the gas densities are relatively low, present challenges to our understanding of the cloud/star formation processes. Also, deciphering the star formation histories of outer stellar disks provide information on the growth of galaxy disks with time and tests current models of disk growth (see, for example, Azzollini *et al.* (2008)). Understanding star formation in the outer stellar disk of galaxies is also important for chemical enrichment as well as the impact of stellar feedback into the low density interstellar medium (ISM) (Thilker *et al.* 2005b). Different proxies are used to trace star formation history in a galaxy. Massive young OB stars embedded in molecular clouds show H_α emission which traces very recent star formation up to $\sim$10 Myr (Knapen *et al.* 2006; Kennicutt 1998). Since tracing CO emission, which is an indicator of molecular hydrogen, is difficult in galaxies beyond the local group, H_α emission is in general compared with the H I column density maps. Both H_α and H I are good tracers to infer the on-going star formation and location of star-forming material. Far-ultraviolet (FUV) radiation which traces the location of massive stars, is used as another proxy to trace star formation in combination with H_α emission (Goddard *et al.* 2010). Hα emission traces present-day star formation, only up to a few Myr ago. On the other hand, ultraviolet (UV) flux and UV colors used in this study, can trace star formation up to a few hundred Myr (Kennicutt & Evans 2012).

The presence of extended UV disk (XUV disk) in many nearby galaxies was confirmed through UV observations by GALEX (Thilker *et al.* 2005a, 2007; Gil de Paz *et al.* 2005; Zaritsky & Christlein 2007; Wilsey and Hunter 2010). It was first discovered in the spiral galaxy M83 by Thilker *et al.* (2005b). Soon after, a few other galaxies with XUV disks well beyond their classical optical radius (R_{25}, the radius at which surface brightness of the galaxy falls below 25 mag/arcsec^2 in the B band), were also found. Star-forming UV knots were identified even up to $4R_{25}$ radius in M83 (Goddard *et al.* 2010). XUV disks are classified into two categories by Thilker *et al.* (2007); those with structured, filamentary UV emission with spiral patterns were classified as XUV I disks and those having large UV emission in the outer disk were classified as XUV II disks. They identified NGC 300 to have a wispy extension of the inner disk at markedly low intensity. Goddard *et al.* (2010) compared FUV, near-ultraviolet (NUV) and H_α measurements for star-forming regions in 21 galaxies, in order to characterize the properties of their disks at radii beyond the main optical radius (R_{25}). They measured H_α flux profile along with UV and noticed that for 10 galaxies, though H_α emission was truncated after R_{25}, the UV emission was detected up to a larger radius, which confirmed that these galaxies have extended outer disks. Zaritsky and Christlein (2007) examined 11 galaxies and found an excess of blue ($(\mathrm{FUV}-\mathrm{NUV})<1, \mathrm{NUV}<25$) sources out to $2R_{25}$ for ∼25% of their sample. Barnes *et al.* (2011) performed an analysis of ultra-deep UV and H_α imaging of five nearby spiral galaxies to study the recent star formation in the outer disk and found UV flux extending up to 1.2–1.4R_{25} for most of them. Goddard *et al.* (2010) used Starburst99 simple stellar population (SSP) model generated NUV magnitudes and (FUV−NUV) colors to determine masses and ages of identified clusters in two XUV disk galaxies, NGC 3621 and M83.

The Sculptor group is among the nearest galaxy groups beyond the Local group (Jerjen *et al.* 1998), which is at a distance of 2 to 5 Mpc. The nearest sub group consists of NGC 55, NGC 300, and possibly two or more known spheroidal companions (Karachentsev *et al.* 2003). NGC 300, the brightest galaxy in the Sculptor group, is nearly isolated, only a dwarf galaxy is found nearby (Tully *et al.* 2006; Karachentsev *et al.* 2003). This galaxy is also a near-optical twin of the Local group galaxy M33. Bland-Hawthorn *et al.* (2005) reported a pure exponential stellar disk up to ∼14.4 kpc (∼2.2R_{25}), which is about 10 disk scale length for NGC 300 while M33 has a disk break at ∼8 kpc (Ferguson *et al.* 2007; Barker *et al.* 2011). The present star formation rate (SFR) in the disk of NGC 300 has been measured and a relatively low value of $\sim 0.08-0.30 M_\odot\ \mathrm{yr}^{-1}$ is estimated by different tracers like Hα emission (Helou *et al.* 2004; Karachentsev & Kaisina 2013), FUV luminosity (Karachentsev & Kaisina 2013), mid-IR (Helou *et al.* 2004) and X-ray (Binder *et al.* 2012). The standard model of the disk galaxy evolution suggests an inside-out growth of the disk, i.e. the inner part of the disk forming earlier than the outer part. Using HST observation of individual stars up to 5.4 kpc, Gogarten *et al.* (2010) concluded an inside-out disk growth in NGC 300 in the last 10 Gyr. Vlajić *et al.* (2009) found an extended stellar disk and an upturn in metallicity gradient at a radius of ∼10 kpc in NGC 300 and concluded that radial mixing or accretion in the outer disk may be the reason behind this change in the metallicity gradient. Gogarten *et al.* (2010) also found a similar metallicity gradient in the inner disk of the galaxy through HST observation and suggested that the probability of radial mixing is very less in NGC 300 because of its low mass. Using HST observation, Hillis *et al.* (2016) studied the star formation history in the past 200 Myr in four different regions of NGC 300 and identified an unbroken young stellar disk at least up to 8 disk scale length. In another study, Rodríguez *et al.* (2016) identified 1147 young stellar groups by studying six different regions in the galaxy and noticed that these groups are mostly present along the spiral arm of the galaxy.

The H I disk of this galaxy is well studied and is found to show some noticeable structures. Puche *et al.* (1990) reported a warp in the H I disk just outside the optical disk. Westmeier *et al.* (2011) used ATCA radio observation and mapped the H I disk of NGC 300 outward to a larger extent. They found a dense inner disk and an extended outer disk of 35 kpc in diameter along the major axis of the galaxy. They also observed an asymmetry in the outer disk, which they speculated to be as due to RAM pressure caused by the interaction between the galaxy and the surrounding inter-galactic medium (IGM).

In this study, we used deep GALEX observations of NGC 300 in both FUV and NUV pass bands to understand the recent star formation in the galaxy. We studied the extent of FUV emission of the galaxy and correlated the overall UV disk structure with optical, H I and infrared emissions. These correlations portray the nature of young star-forming regions in the galaxy. We generated the radial profile for surface luminosity density and SFR density to understand the nature of UV emission. We also identified several UV sources in the outer disk of

the galaxy and estimated their mass and age with the help of synthetic UV magnitudes/colors and explored their spatial distribution.

The paper is arranged as follows. The data are presented in Section 2, the background and foreground source subtraction is discussed in Section 3, the reddening and metallicity in Section 4, the models are given in Section 5, the analysis in Section 6 followed by a discussion and summary in Sections 7 and 8 respectively.

2. Data

The archival GALEX images of NGC 300, with a total exposure time of 12987.6 s (NUV and FUV) were obtained from the MAST data archive. GALEX has two channels, far-UV (1350–1750) Å and near-UV (1750–2800) Å with a resolution of 4.5–6″. These observations were obtained between 2004-10-26 to 2004-12-15, and the Image ID is 3073040579138954826 (tile name GI1_061002_NGC0300). We used images as well as the catalog of sources produced by the GALEX data pipeline (Morrissey *et al.* 2007) for the whole 1.25° field-of-view. The catalog contains 19289 identified sources within the total field-of-view. Out of these, we found 6554 sources to have both FUV and NUV detection. The catalog provides apparent magnitudes of sources in both the FUV and the NUV band along with their RA and DEC.

We have also used Australia Telescope Compact Array (ATCA) and Galactic All-Sky Survey (GASS) combined H I data of NGC 300 for correlating with the UV properties. The data cube, containing 53 image files was obtained from Westmeier *et al.* (2011). We combined all the images using IDL and obtained a complete H I map of the galaxy. In order to compare our results with optical and infra-red, we have used Digitized Sky Survey (DSS) blue band, Infrared Array Camera (IRAC) 3.6 μm and Multiband Imaging Photometer (MIPS) 24 μm images of the galaxy obtained from the NASA/IPAC Extragalactic Database (NED).

3. Background and foreground sources

It is very important to exclude background galaxies and foreground stars from the identified source catalog. Since the galaxy NGC 300 is located at a high galactic latitude ($b \approx -79°$) (Vlajić *et al.* 2009), very less number of foreground stars are expected to be present in the field. In order to remove background sources, we divided the whole GALEX tile into two regions having equal area which are shown in Figure 1. One is the inner circular region (i.e. galaxy region) having a radius of 25.8 arcmin and another is the outer annular region (i.e. field region) with an inner and outer radii of 25.8 and 36.5 arcmin respectively. We assumed all the sources present in the outer annular region as background contaminants and used them to remove background sources present in the inner circular region by a statistical technique. We constructed FUV vs. (FUV−NUV) color magnitude diagrams (CMD) for sources present in both the galaxy region and the field region (Figure 2). We considered each source in the field CMD and identified its nearest counterpart in the galaxy CMD and then removed it from the inner circular region. In order to do this, we constructed a grid of [magnitude, color] bins with different sizes, starting from [$\triangle$FUV, $\triangle$(FUV − NUV)] = [0.01, 0.01] and reaching up to a maximum of [0.5, 0.5]. The number of sources present in the inner region and the field region are 3880 and 2674 respectively. Following the above mentioned technique, we removed 2507 number of sources from the galaxy region as background contamination and are left with 1373 sources. We have shown the CMD for 1373 sources in Figure 3a. Since the fraction of background contaminants increases with decreasing brightness value, we have further excluded sources fainter than 23 mag in the FUV band assuming them to be background galaxies. The foreground stars

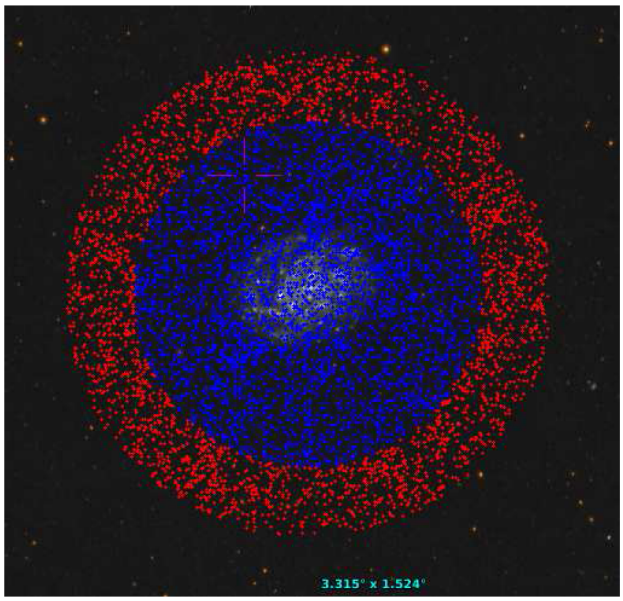

Figure 1. The identified sources (detected in both the FUV and NUV bands) are over plotted on GALEX image of NGC 300. The inner circular region, containing the blue points, is considered as the galaxy and the outer annular region with red points is assumed as the field region.

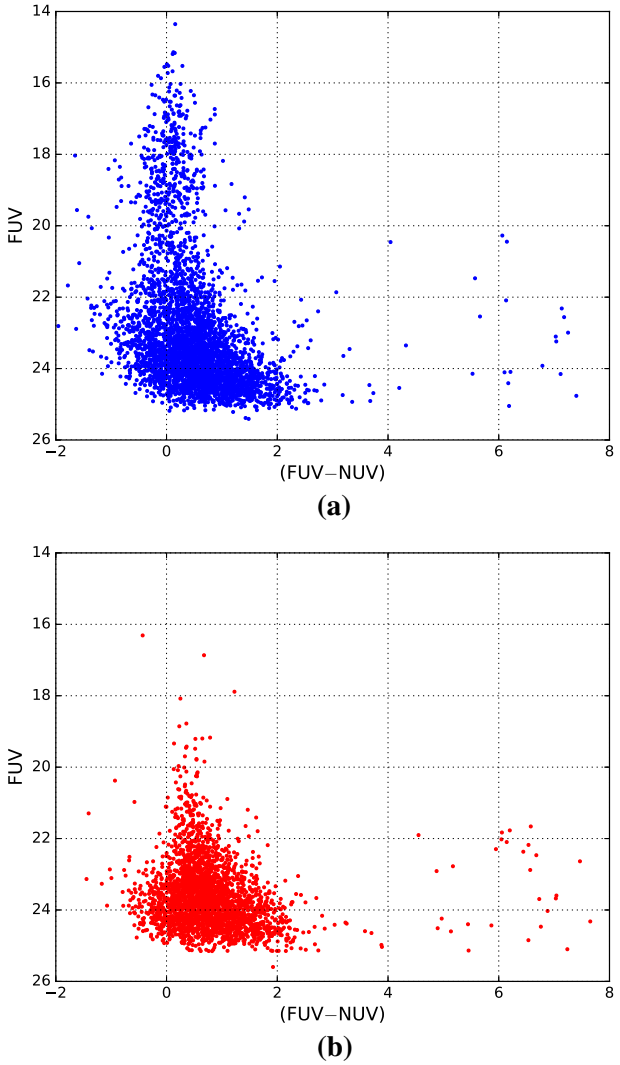

Figure 2. **(a)** The FUV vs. (FUV−NUV) CMD for the galaxy region (blue points in Figure 1) is shown and **(b)** the CMD for the outer field region (red points in Figure 1) is shown.

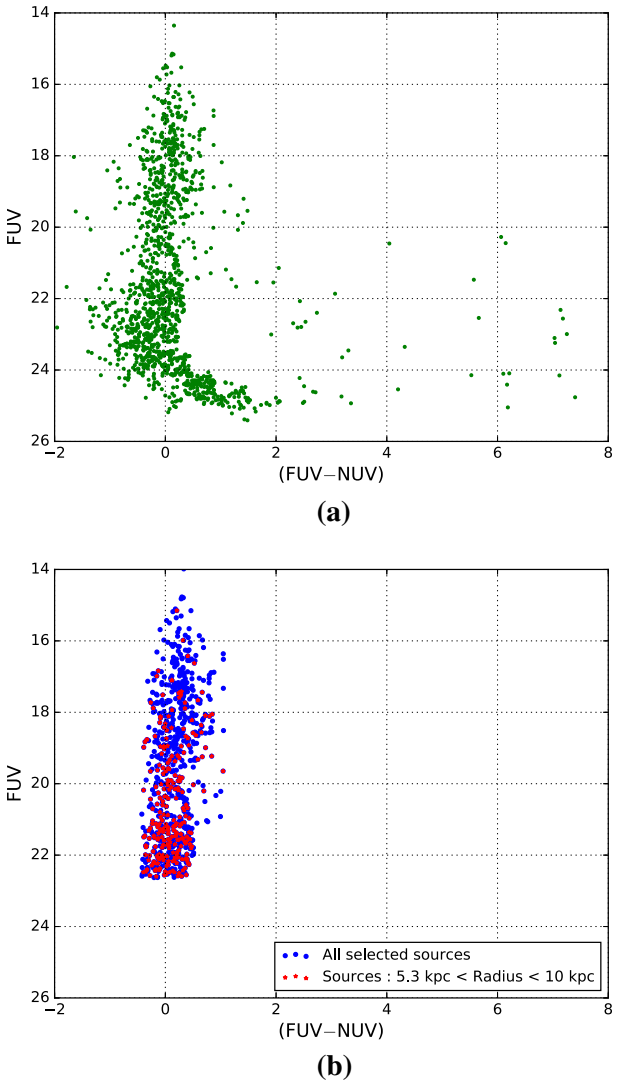

Figure 3. **(a)** The FUV vs. (FUV−NUV) CMD of the sources remaining in the galaxy region after performing background subtraction. **(b)** The CMD of 742 UV sources (reddening and extinction corrected) which are finally considered as part of the galaxy. The sources marked with the red star are present in the outer disk between radius 5.3 kpc to 10 kpc.

are expected to have a larger (FUV−NUV) color. In the study of extended disks of several nearby galaxies using GALEX data, Goddard *et al.* (2010) considered only sources with $(\mathrm{FUV}-\mathrm{NUV}) < 1.5$ to exclude foreground and background sources. We treated sources with $(\mathrm{FUV}-\mathrm{NUV}) > 1.0$ as not part of the galaxy and excluded them. The remaining sources are corrected for reddening and extinction (discussed in Section 4). The sources with corrected $(\mathrm{FUV}-\mathrm{NUV}) < -0.43$ (∼7% of the remaining sources) are also excluded since their color value is outside the model range. Finally, we are left with 742 sources in the galaxy region and we consider them as candidate UV sources of the galaxy. The reddening and extinction corrected CMD for these 742 selected UV sources are shown in Figure 3b. Since our main interest is to study the outer disk of the galaxy, out of these 742 UV sources, we selected 261 sources which are present between the radii 5.3 kpc (optical radius of NGC 300 (Faesi *et al.* 2014)) to 10 kpc, for our analysis. These 261 sources are shown in red in Figure 3b.

We have also estimated the number of background galaxies in both the GALEX FUV and NUV filters following the study of Xu *et al.* (2005). For the magnitude range 14.2 to 23.7, the estimated number of background galaxies are $0.7/\mathrm{arcmin}^2$ and $1.4/\mathrm{arcmin}^2$ respectively in the FUV and NUV bands. Through our statistical method, we have excluded 2507 sources (∼93% of the

total field sources) from the galaxy region, which corresponds to a density of $\sim 1.2/\text{arcmin}^2$, similar to the numbers provided above. We therefore conclude that our sample has negligible contamination due to background as well as foreground sources.

4. Reddening and metallicity

We corrected reddening and extinction to estimate the intrinsic (FUV–NUV) color and both the FUV and NUV magnitudes for all selected sources. To study the outer stellar disk of NGC 300, Vlajić *et al.* (2009) considered a foreground reddening $E(B-V) = 0.011 - 0.014$ mag. The foreground reddening given in the GALEX catalog for the field of NGC 300 is also very low ($E(B-V) \approx 0.01$). Apart from this, interstellar extinction also contributes to reddening inside the disk of a galaxy. Using HST observation, Rodríguez *et al.* (2016) studied different regions (from inner to outer disk) of NGC 300 by considering a constant reddening of $E(B-V) = 0.075$ mag. In our study, we also adopted this reddening value throughout the galaxy. The following conversion rules are used to calculate E(FUV–NUV), A(FUV) and A(NUV) from $E(B-V)$:

$$E(\text{FUV}-\text{NUV}) = R(\text{FUV}-\text{NUV})E(B-V), \quad (1)$$

$$A(\text{FUV}) = R(\text{FUV})E(B-V), \quad (2)$$

$$A(\text{NUV}) = R(\text{NUV})E(B-V). \quad (3)$$

We adopted the value of reddening coefficients from Yuan *et al.* (2013). Using the standard pair technique over a large sample of galactic stars, they estimated the values of R(FUV–NUV), R(FUV) and R(NUV) to be -2.35, 4.89 and 7.24 respectively for GALEX filters. The estimated values of E(FUV–NUV), A(FUV) and A(NUV) are -0.18 mag, 0.37 mag and 0.54 mag respectively. These are used to correct color and magnitude of all the sources. We used the reddening corrected color (FUV−NUV) and extinction corrected magnitude (FUV, NUV) throughout our analysis. In order to estimate different parameters of the detected sources, we adopted $Z = 0.02$ as the present day metallicity of the star-forming regions from the study of supergiant stars in NGC 300 done by Gazak *et al.* (2015) and Kudritzki *et al.* (2008).

The parameters of the galaxy are presented in Table 1. We calculated the inclination-corrected galactocentric distance (in kpc) for each source by considering the galaxy center as $\alpha_0 = 13.722833$, $\delta_0 = -37.684389$, distance $d = 1.9$ Mpc, inclination $i = 42.3°$ and position angle (PA) of the major axis $\theta = 109°$.

5. SSP model

We used the Starburst99 SSP model (Leitherer *et al.* 1999) to generate diagnostic diagrams for studying the young star-forming regions of the galaxy NGC 300. It is a spectrophotometric SSP model primarily used to understand the active star-forming regions of a galaxy. Mondal *et al.* (2018) employed this model to estimate the masses of several compact star-forming regions present in a dwarf irregular galaxy WLM. Faesi *et al.* (2014) used this model to estimate the mass and age of H_α regions present in the inner disk of the NGC 300. This was also used by Goddard *et al.* (2010) to generate synthetic model grids. They compared these model grids with the GALEX FUV and NUV data of galaxy M31 and NGC 3621 to estimate mass and age of clusters. Dong *et al.* (2008) used the Starburst99 model to generate UV-MIR spectral energy distributions (SEDs) and obtained a constraint on the mass and age of clusters in the extended outer disk of M83.

Table 1. Properties of NGC 300.

Property	Value	References
RA	00:54:53.4	Skrutskie *et al.* (2006)
DEC	–37:41:03.7	Skrutskie *et al.* (2006)
Morphological type	SA(s)d	de Vaucouleurs *et al.* (1991)
Distance	1.9 Mpc	Rizzi *et al.* (2006)
Inclination	42.3°	Puche *et al.* (1990)
PA of major axis	109°	de Vaucouleurs and Page (1962)
Mass	$2.9 \times 10^{10} M_\odot$	Westmeier *et al.* (2011)
R_{25}	5.3 kpc	Faesi *et al.* (2014)
Optical scale-length (R_d)	2.1 kpc	Carignan (1985)

Table 2. Starburst99 model parameters.

Parameter	Value
Star formation	Instantaneous
Stellar IMF	Kroupa (1.3, 2.3)
Stellar mass limit	0.1, 0.5, $120M_{\odot}$
Cluster mass range	$10^3 M_{\odot}$–$10^7 M_{\odot}$
Stellar evolution track	Geneva (high mass loss)
Metallicity	$Z = 0.04, 0.02, 0.008, 0.004, 0.001$
Age range	1–900 Myr

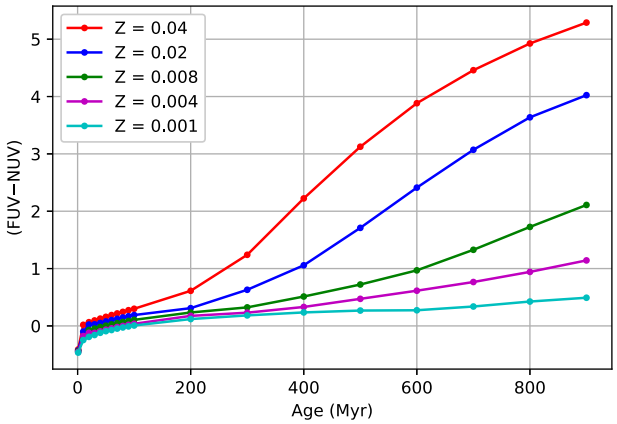

Figure 4. Starburst99 model generated (FUV−NUV) color as a function of age (Myr). Different curves are for five different metallicities (Z). For the 1–100 Myr range, the age interval is 10 Myr and after that interval, it is 100 Myr for age up to 900 Myr. The cluster mass considered is $10^6 M_{\odot}$.

We acquired Starburst99 model data for the chosen set of parameters given in Table 2. Assuming the star formation to be instantaneous, we considered the IMF value as 1.3 (for $0.1M_{\odot}$ to $0.5M_{\odot}$), 2.3 (for $0.5M_{\odot}$ to $120M_{\odot}$) (Kroupa IMF) (Kroupa 2001) with stellar mass limit as $M_{\rm low} = 0.1M_{\odot}$ and $M_{\rm up} = 120M_{\odot}$. We considered the total mass of the cluster in the range $10^3 M_{\odot} - 10^7 M_{\odot}$. The nebular radiation for the total integrated light are also taken into account.

5.1 *Age*

We calculated (FUV–NUV) color for ages varying from 1 to 900 Myr with five different metallicities ($Z = 0.04$, 0.02, 0.008, 0.004, 0.001). The diagnostic curves are shown in Figure 4.

Figure 4 shows the following:

(1) For a fixed metallicity, (FUV–NUV) color increases with age.
(2) Change in color for the entire age range increases with metallicity.

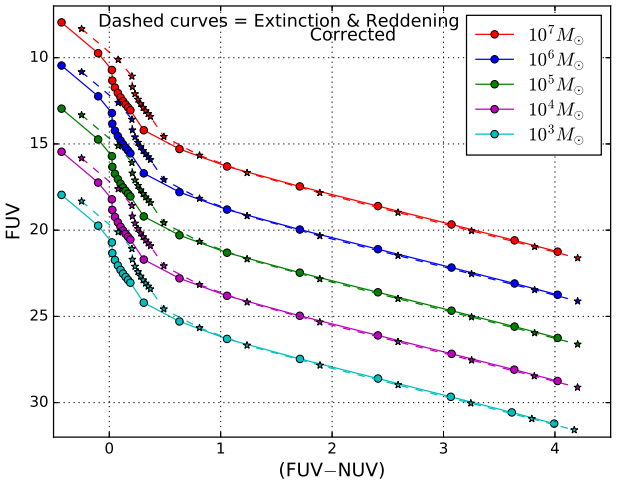

Figure 5. Starburst99 model generated FUV *vs.* (FUV−NUV) CMD for simple stellar population. Different curves signify five different total cluster masses ($10^7 M_{\odot}$, $10^6 M_{\odot}$, $10^5 M_{\odot}$, $10^4 M_{\odot}$, $10^3 M_{\odot}$). The points shown in each curve are for different ages starting from 1 Myr to 900 Myr (increasing along the color axis) with the same age interval chosen in Figure 4.

For a given metallicity, we will be able to calculate the age of any source from its (FUV–NUV) color with the help of this model grid. We have considered the age range as 1–900 Myr. It should be noted that (FUV–NUV) color is not sensitive to estimate the age beyond ∼500 Myr because of the substantial drop in the far-UV flux.

5.2 *Mass*

We also produced model grids for FUV magnitude as a function of (FUV–NUV) color. The model fluxes and the corresponding magnitudes are estimated by adopting a distance of 1.9 Mpc for NGC 300 (Rizzi *et al.* 2006). Keeping all model parameters unchanged, we considered five different values for the total cluster mass ($10^7 M_{\odot}$, $10^6 M_{\odot}$, $10^5 M_{\odot}$, $10^4 M_{\odot}$, $10^3 M_{\odot}$) for a fixed metallicity of $Z = 0.02$, which is adopted for NGC 300, to generate Figure 5.

Figure 5 shows the following:

(1) Older clusters have redder (FUV–NUV) color irrespective of mass.
(2) For a given age (or equivalently, color), clusters become more brighter with increasing mass.

These model grids can be used to calculate both age and mass of sources from their color and magnitude for $Z = 0.02$.

Table 3. Details of flux and magnitudes for contours in the FUV map shown in Figure 6.

FUV magnitude range (extinction corrected)	Flux_{FUV} (erg/s/cm^2/Å) (extinction uncorrected)	Contour color
<20	$>33.6 \times 10^{-15}$	Blue
>20 and <21	$13.3-33.6 \times 10^{-15}$	Green
>21 and <23	$0.21-13.3 \times 10^{-15}$	Red

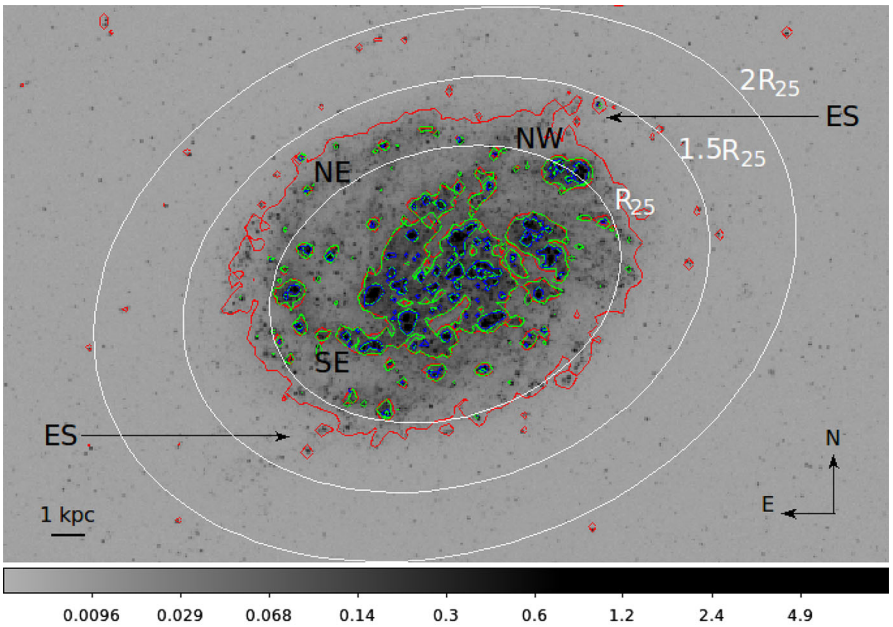

Figure 6. The background figure is the binned 960 × 960 pixel FUV image of NGC 300 with different contours plotted for different limits of FUV flux value as mentioned in Table 3. The blue contours represent the brightest (hence massive) regions of the galaxy. The gray scale of the image denotes counts per second per pixel. The ellipses shown in the figure signify R_{25}, $1.5R_{25}$ and $2R_{25}$ galactocentric distances respectively. Two extended structures (ES) are also shown by arrow.

6. Analysis

6.1 *FUV disk of NGC 300*

In order to identify large massive star-forming complex of NGC 300, we produced a 960 × 960 pixel image from the 3840 × 3840 pixel GALEX FUV image by binning 4 × 4 pixels of original image as one single pixel. Each pixel of the binned image has an area coverage of $\sim 6 \times 6$ arcsec^2 ($\sim 55 \times 55$ pc^2). The resolution of the image is degraded such that the pixel size becomes comparable to the average size of the young stellar groups in the NGC 300 identified by Rodríguez *et al.* (2016). Since far-UV radiation is mainly contributed by massive young stars, we considered the image in the FUV filter for this purpose. To understand the distribution of star-forming regions, we created different contours by fixing the lower and the upper limit of fluxes which are given in Table 3. The FUV image with different contours is shown in Figure 6. The massive star-forming complexes of NGC 300 are picked up by the blue contours created for pixel brighter than 20 magnitude (i.e. $\text{Flux}_{\text{FUV}} > 33.6 \times 10^{-15}$ erg/s/cm^2/Å). The two main spiral arms of the galaxy, one along the north-west (NW) and another along east to north-east (NE) are found to have massive star-forming complexes which all together follow the spiral structure. Almost all of these complexes are found to be present within the optical radius (R_{25}) of the galaxy. The green contours, signifying relatively less bright regions, are found around each of the blue contoured regions. The red contours, generated for pixels fainter than 21 magnitude and brighter than 23 magnitude, trace the extended structure of the FUV disk nearly up to a radius of 7 kpc. The north-eastern spiral arm which do not have much massive complexes, is mainly covered by this

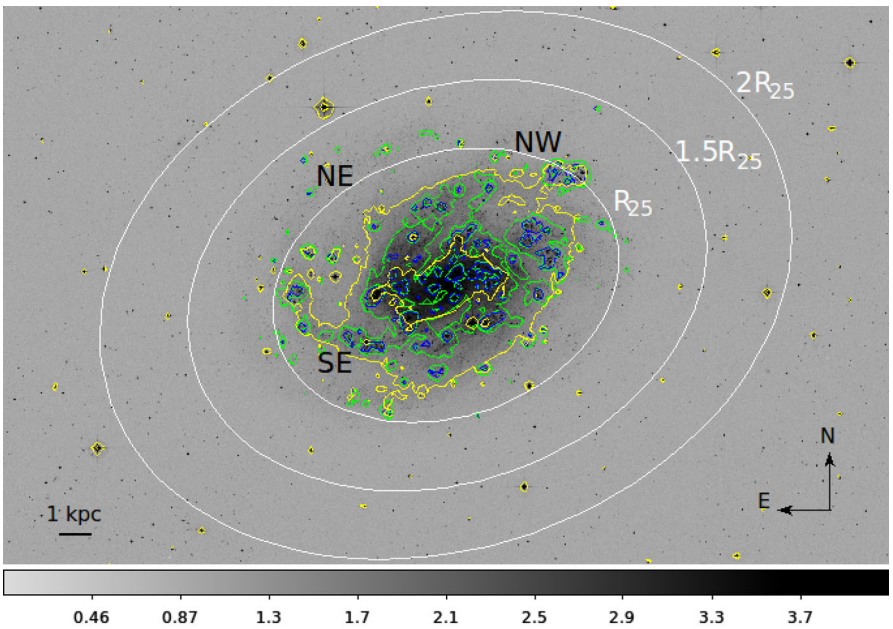

Figure 7. The background figure shows the DSS optical image of NGC 300. The yellow contoured region represents the main optical disk of the galaxy. Blue and green contours are the same as shown in Figure 6.

red contour. We do see two extended structures along the major axis (south-east (SE) to north-east (NW)) of the galaxy which are mainly picked up by the red contours. The regions covered by the red contour in the east and northern parts, extend beyond the optical radius (R_{25}) of the galaxy. Therefore, NGC 300 has an extended UV disk with relatively less massive star-forming complexes when compared to the inner disk.

6.2 *Correlation with optical image*

As the young massive stars have a large continuum flux in the UV, when compared to that in the optical, a correlation between the UV and the optical emission will eventually help to trace the young star-forming regions. In order to correlate the FUV disk of NGC 300 with the optical disk, we have over plotted the blue and green contours of Figure 6 on the DSS optical image of the galaxy in Figure 7. The yellow contour in Figure 7 displays the main part of the optical disk of the galaxy. It is noticed that the massive complexes identified in the GALEX FUV image of NGC 300 (blue and green contour) correlate well with the optical disk structure (yellow contour) of the galaxy. It is to be noted that the optical emission arising from the north-eastern spiral arm of the galaxy is very low compared to other regions of the galaxy, whereas in the FUV image (Figure 6), we can clearly notice the spiral arms and the extended structures present in the outer disk of the galaxy. Therefore, the extended disk, identified in UV, is not easily noticeable in the optical image of the galaxy.

6.3 *Correlation with H I*

In order to correlate the distribution of the young star-forming regions and H I column density of the galaxy, we over plotted the FUV contours of Figure 6 on the H I map in Figure 8a. The H I density contours, generated for a higher threshold value, are shown in white in the same figure. It is noticed that the extent of the detected FUV disk of the galaxy is well within the dense H I disk. H I contour map shows a large compression of gas in the south-eastern part of the galaxy. Westmeier *et al.* (2011) found that the south-eastern side showed a distinctive plateau, followed by a sudden and steep drop in the column density of the H I disk, which is not found in the north-western side. The UV sources which are present along the north-eastern spiral arm of the galaxy are also found to coincide with the dense H I contours (Figure 8b). A kink in the density contour is also seen in the northern direction and it coincides with the extended structure identified in the source distribution. The extended features noticed along the south-east and north-west direction also follow the extended density contour of H I.

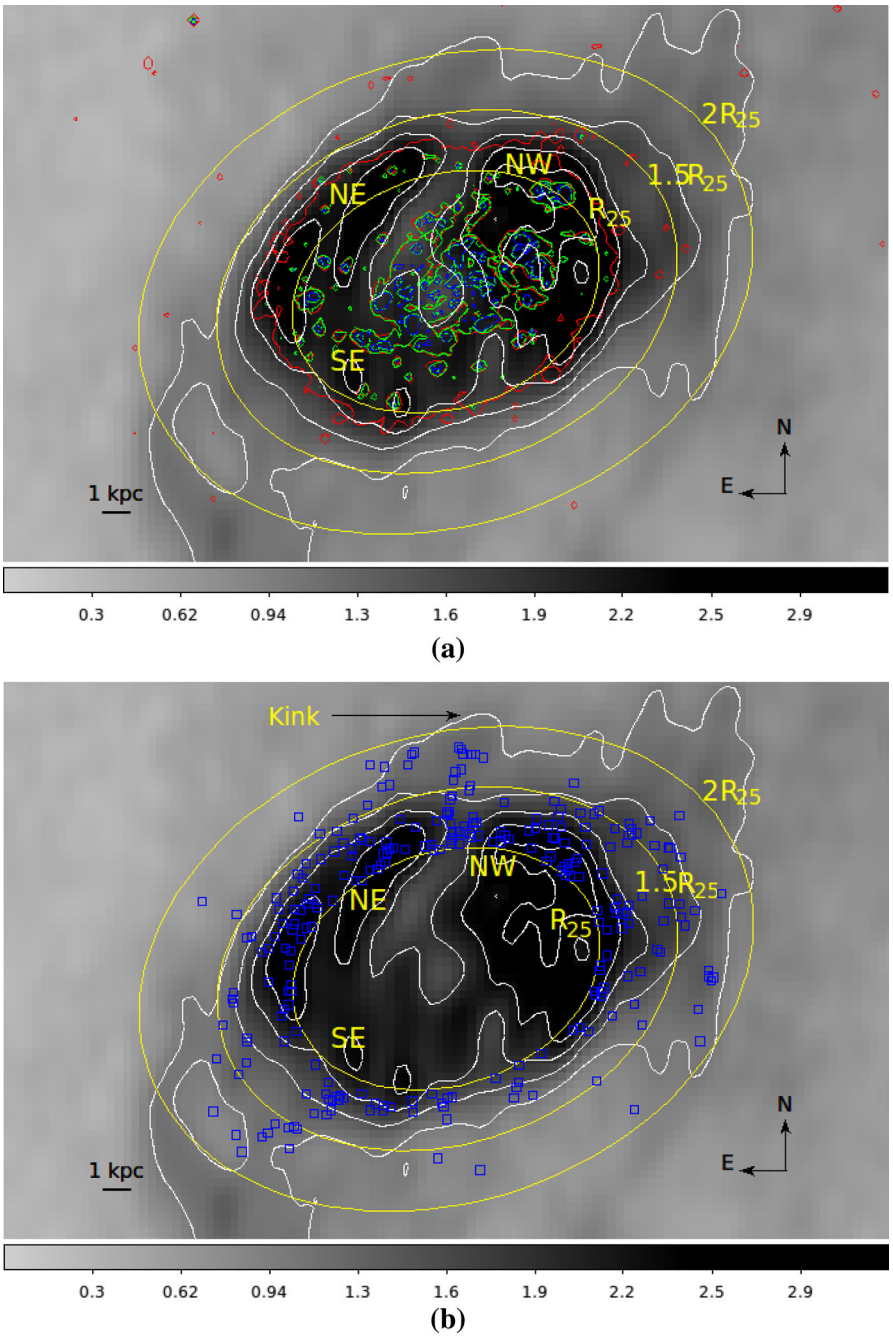

Figure 8. The H I density contours are shown in white on the background H I density map of NGC 300 in both the figures. The unit of the gray scale is Jy/beam. The blue, green and red contours shown in (a) are the same as in Figure 6. In (b), we have shown the distribution of the UV sources (blue points) present in the outer disk (between 5.3 kpc and 10 kpc) of NGC 300.

6.4 *Correlation with 24 μm infrared image*

The star-forming regions of the galaxy NGC 300 are found to have strong 24 μm infrared emission (Helou *et al.* 2004). Since the dust present in the star-forming regions gets heated by the FUV photons originating from the massive stars which in turn produces radiation in 24 μm, it is expected that the massive star-forming complexes detected in the FUV image of NGC 300 should also show emission in 24 μm. In order to verify this, we over plotted the blue contour (of Figure 6), signifying massive star-forming complex, on the infrared 24 μm image of the galaxy in Figure 9. The red contours shown in the figure indicate the regions with intense 24 μm emission. It is noticed that for the inner disk, both the blue and red contours show a good spatial

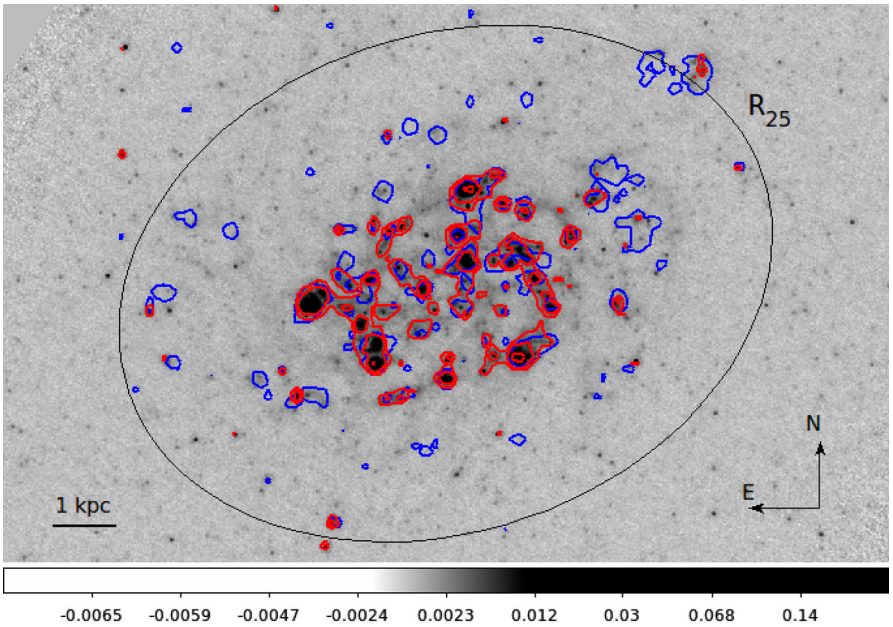

Figure 9. The MIPS 24 μm image of NGC 300 is shown in the background with red contours indicating regions with intense infrared emission. The same blue contours of Figure 6 are also shown. The unit of the gray scale is MJy/sr.

correlation which signifies the location of active star-forming regions in NGC 300. We also note that a few FUV emission regions located within R_{25}, do not have corresponding 24 μm emission. This may be due to a variety of reasons such as difference in resolution and sensitivity of the detections in these wavelengths, reduced dust in the outer regions, the presence of a few possible not-so-young star-forming regions without dust, etc.

6.5 *Luminosity density profile*

The emission from stellar population of different ages peaks in different wavelengths. The older populations show a significant emission in the optical and infrared bands whereas the emission from younger populations mainly peak in the UV. In order to trace the disk of NGC 300 in different wavelengths, we produced normalized surface luminosity density profiles of the galaxy in different wavebands which are shown in Figure 10. These profiles depict the nature of the galaxy disk in different wavelengths. The disk scale-length ($R_{\rm d}$) of NGC 300 is reported to be 2.10 kpc and 1.47 kpc respectively in the optical B band and the infrared I band (Carignan 1985; Kim *et al.* 2004). These two independent measurements highlight that the disk is more extended in shorter wavelengths. We used GALEX FUV and NUV, DSS optical B band and infrared 3.6 μm IRAC images to estimate the disk scale-length by fitting an exponential curve to each of the observed

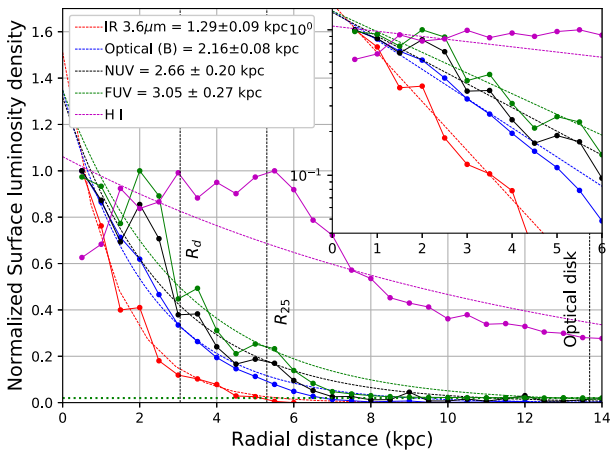

Figure 10. The normalized surface luminosity density profiles of NGC 300 in different wavebands are shown in different colors. The *solid* lines denote the observed profiles whereas the *dashed* lines of the same color show the fitted exponential profiles. Three vertical black dashed lines are plotted to show the FUV scale-length (R_d) (our study), optical radius (R_{25}) and the extended optical disk of the galaxy from Bland-Hawthorn *et al.* (2005). The horizontal dotted green line represents the FUV background. In the inset, we have shown all the observed and fitted profiles in logarithmic scale up to radial distance of 6 kpc.

profiles, shown in Figure 10 in different colors. The measured values of the scale-length are 1.29 ± 0.09 kpc, 2.16 ± 0.08 kpc, 2.66 ± 0.20 kpc and 3.05 ± 0.27 kpc respectively for infrared, optical B band, NUV and FUV.

This suggests that the disk of the NGC 300 gradually extends to larger radii from longer to shorter wavelength. The distribution of younger populations, traced by the FUV disk, is found to be more extended than the rest. Thus this confirms the presence of the XUV disk in the galaxy NGC 300. The average FUV background, estimated from the flux measured between radii 14 and 15 kpc is shown in green dotted line. The observed FUV luminosity density profile nearly converges to the background level at a radius of ∼12 kpc. Therefore, we conclude that the disk of the NGC 300 is extended at least up to ∼12 kpc. We have also shown the radial H I column density profile of the galaxy in the same figure. The behaviour of this profile is found to be different than the rest. Instead of an exponential nature like other bands, it shows a dip in the central part with a gradual increase up to radius ∼5.5 kpc. Beyond this radius, the profile drops down slowly in the outer disk. We did not show the Hα profile because the image available for that in the NED has a radial coverage of around 4 kpc, which is less than the optical radius of the galaxy.

6.6 *Star formation rate*

To estimate the SFR of NGC 300, we considered a radius of 10 kpc ($1 \sim 2R_{25}$) and measured the total flux within that from the GALEX FUV image. This flux is corrected for extinction and background as discussed in the previous section and further converted to magnitude. We used equation (4) from Karachentsev & Kaisina (2013), where $\mathrm{mag_{FUV}}$ denotes the background and extinction corrected magnitude and D is the distance to the galaxy in Mpc, to calculate the SFR ($M_\odot$/yr) of the galaxy. The total SFR integrated up to a radius of 10 kpc for NGC 300 is found to be 0.46 $M_\odot$/yr, which nearly matches with the earlier estimate of 0.30 $M_\odot$/yr by Karachentsev & Kaisina (2013). To generate the radial profile of the SFR density ($M_\odot$/yr/kpc^2), we similarly considered annuli of width 0.5 kpc from the center to a radius 10 kpc and measured the background and extinction corrected FUV magnitude per kpc^2 in each individual annuli. We used equation (4) to estimate the SFR for each annuli and plotted radially in Figure 11. The profile shows that the central 2 kpc of the galaxy shows high SFR density. After that it starts decreasing and becomes a little stable within the radius 5.5 kpc. Beyond this radius, the SFR density becomes very small compared to the inner disk. In a study of NGC 300 using HST data, Gogarten *et al.* (2010) calculated the radial SFR density ($M_\odot$/yr/kpc^2) for different age ranges. They used three HST ACS fields oriented as a radial strip from the center to outside of the galaxy in the western part. These fields thus cover a limited part of the galaxy's inner disk. Our study instead considered the whole galaxy disk observed by GALEX to estimate the azimuthally averaged radial SFR density profile of NGC 300. Both these measurements have different area coverage and hence values are expected to be different. In order to check only the nature of the radial profile from both the studies, we have plotted the values from Gogarten *et al.* (2010) for the age range 4–80 Myr (Figure 11, red curve), after scaling it to our estimations. The plot highlights that though HST covers a specific part of the disk, the nature of the radial profile closely follows that estimated for the whole disk with GALEX in this study.

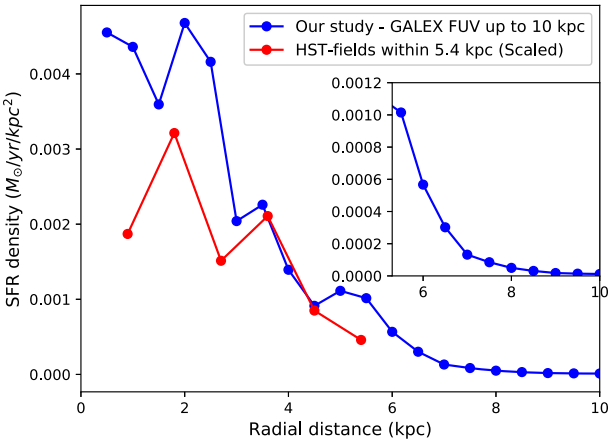

Figure 11. The radial profile of the SFR density ($M_\odot$/yr/kpc^2) is shown up to a radius 10 kpc (blue curve). The red curve shows the scaled value of the SFR density ($M_\odot$/yr/kpc^2) as calculated through an HST study by Gogarten *et al.* (2010). The radial profile of the SFR density between radii 5.3 kpc and 10 kpc is shown in the inset.

$$\log(\mathrm{SFR_{FUV}}(M_\odot/\mathrm{yr})) = 2.78 - 0.4 * \mathrm{mag_{FUV}} + 2\log(D). \quad (4)$$

6.7 *Age estimation of UV sources*

The diagnostic diagram shown in Figure 4 can be used to estimate the age of a source from its (FUV–NUV) color for a given metallicity. As NGC 300 is observed to have solar metallicity, we considered the blue curve ($Z = 0.02$) in Figure 4 to estimate the age of the identified UV sources. The sources detected in the inner disk have crowding issue. Because of the poor spatial resolution of GALEX, a combination of multiple sources in the inner disk can appear like a single source. Whereas in the outer disk of the galaxy, artefact due to crowding is much reduced. Also, out of 742 we selected

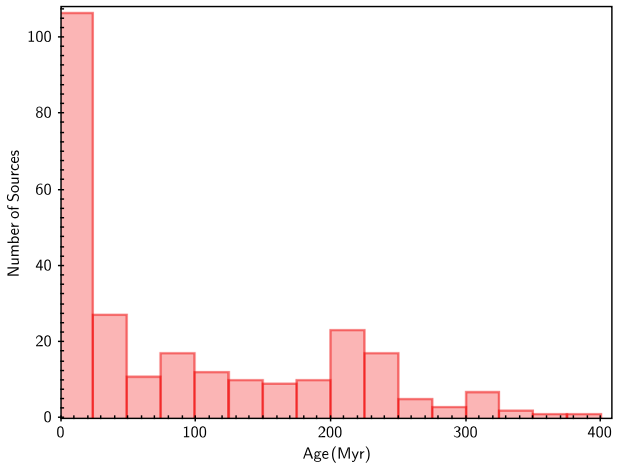

Figure 12. Age histogram of all the selected UV sources between radius 5.3 kpc and 10 kpc.

261 sources having galactocentric distance greater than 5.3 kpc and less than 10 kpc for our study. We do not consider sources beyond 10 kpc for contaminants might be more in the far outer disk. We used the reddening corrected observed color of these 261 UV sources and interpolated it with the model data (blue curve) to estimate their ages within the range 1 to 400 Myr. In Figure 12, we have shown the age histogram for these selected UV sources. The figure signifies that the outer disk of the NGC 300 has a large number of young sources with age less than 25 Myr.

6.8 *Spatial age distribution of UV sources*

In order to visualize the spatial age distribution of these 261 selected UV sources, we separated them into two groups, one as the young group (age $<$ 25 Myr) and another one a relatively older group (age $>$ 25 Myr). The sources in each groups are then over plotted on the GALEX FUV image in Figure 13. 60% of the sources with age $<$ 25 Myr are found to be present between PA 0–180° whereas 40% are present between PA 181–360°. In case of sources older than 25 Myr, the scenario is exactly opposite to this. Majority of the younger sources (age $<$ 25 Myr) are found to be present along the north-eastern spiral arm of the galaxy (Figure 13a). The extended part of a spiral arm seen in the western part of the galaxy are found to be populated by most of the older sources (Figure 13b). The elongated distribution of sources along the major axis of the galaxy (south-east to north-west) is seen only for the older sources.

6.9 *Mass estimation of UV sources*

The SSP models as shown in Figure 5 suggest that for a given color (equivalently age), the FUV magnitude changes with cluster mass. We plotted 742 selected sources on the simulated figure (shown in Figure 5) and displayed in Figure 14. This figure helps us to estimate mass for each selected source. We performed a linear interpolation between the two nearest model-generated magnitude values to estimate the mass of a source corresponding to the observed extinction corrected magnitude. As our study aims to explore the outer disk only, we estimated mass for 261 sources present between radii 5.3 kpc to 10 kpc ($1 \sim 2R_{25}$) of the galaxy. The histogram of the estimated masses of all these 261 sources is shown in Figure 15. The figure clearly shows that majority of the sources present in the outer disk of the galaxy have mass less than $10^5 M_\odot$. The sources with masses below $10^3 M_\odot$ are not shown in Figure 15 as their measured value is not accurate due to the lower limit of the model mass range (Figure 5). The sources identified in the inner disk are relatively more massive. There can be an artefact of assuming multiple sources as a single one due to crowding in the inner disk.

6.10 *Spatial mass distribution of UV sources*

In order to map the mass distribution of UV sources in the outer disk, we have separated the selected sources into three groups, such as high mass ($M > 10^5 M_\odot$), intermediate mass ($10^3 M_\odot < M < 10^5 M_\odot$) and low mass ($M < 10^3 M_\odot$) and over plotted them on GALEX FUV image in Figure 16. The massive sources are small in number and are mainly found near the inner disk of the galaxy (Figure 16a). The extended arm in the north-west direction is found to have a few massive sources. We see this arm to be extended more in the outer disk in Figure 16b, where it is populated by intermediate mass sources. The inner part of the north-eastern spiral arm is also found to have intermediate mass sources. The low mass sources, which are not shown in Figure 15, are mostly seen in the outer part of the north-eastern spiral arm (Figure 16c). We also noticed two clumps of low mass UV sources, one in the northern part and another in the south-eastern part of the galaxy. Figure 16 conveys that the outer disk of NGC 300 has mostly formed low and intermediate mass sources (~86% of the selected sample) in the last few hundred Myr.

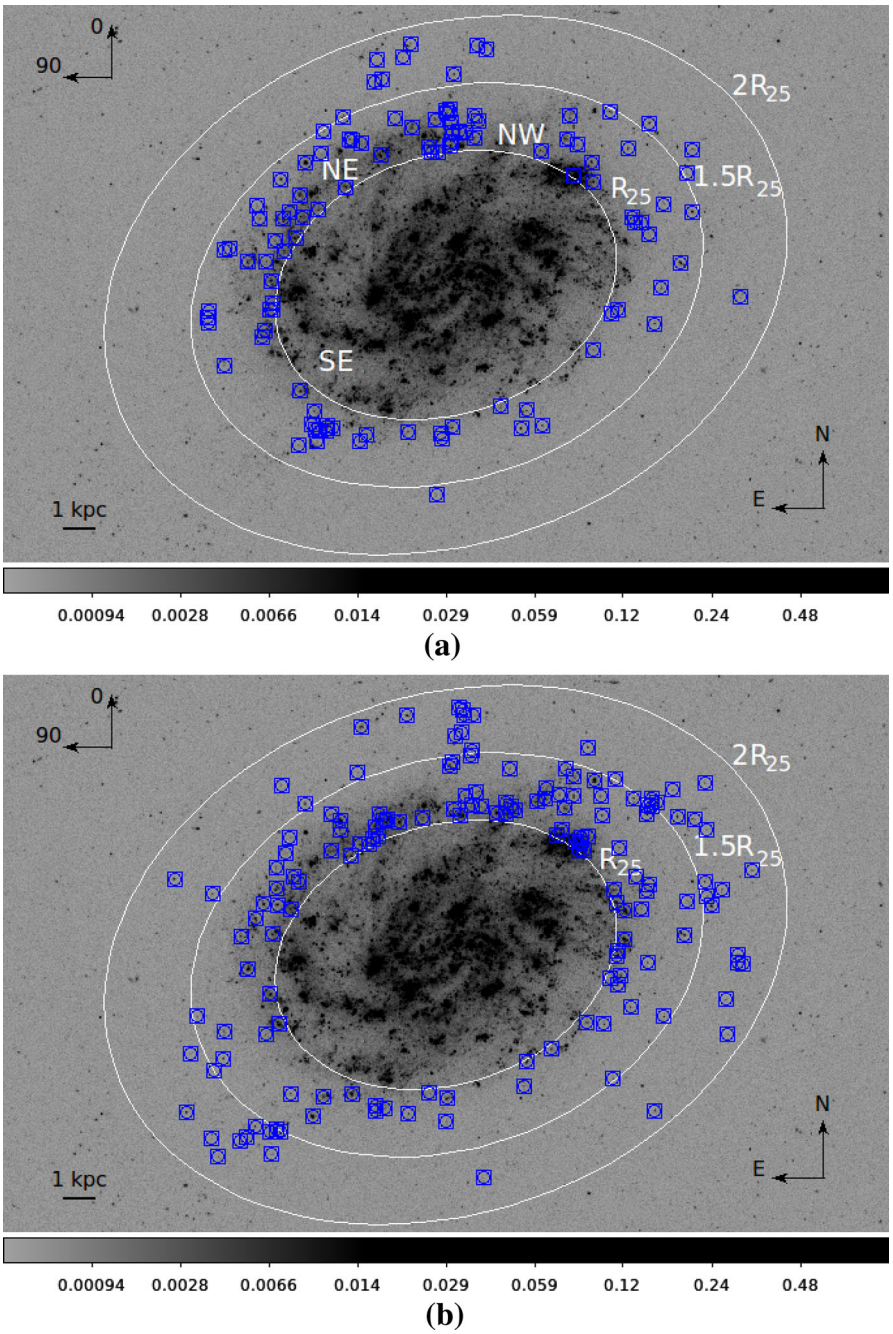

Figure 13. The selected UV sources (blue squares) in the outer disk are over-plotted on the GALEX FUV image of the galaxy. **(a)** The spatial position of younger sources (age < 25 Myr) and **(b)** the relatively older sources (age > 25 Myr) are shown. The reference PA is shown in the top left corner.

7. Discussion

Understanding the nature of star formation in the outer part of the disk galaxies is an important ingredient to the evolution of the galaxy (Barnes *et al.* 2011). As the outer disks of galaxies have lower gas density, lower metallicity and lower dust content, altogether it offers an extreme environment to explore the characteristics of star formation (Zaritsky & Christlein 2007; Barnes *et al.* 2011). Detection of young star-forming complex in the outer disk is also important to test the star formation threshold. The young and massive OB stars contribute a substantial amount of far-UV radiation which can trace the location of the young star-forming regions in a galaxy. The key aim of this study was to decipher the FUV disk properties

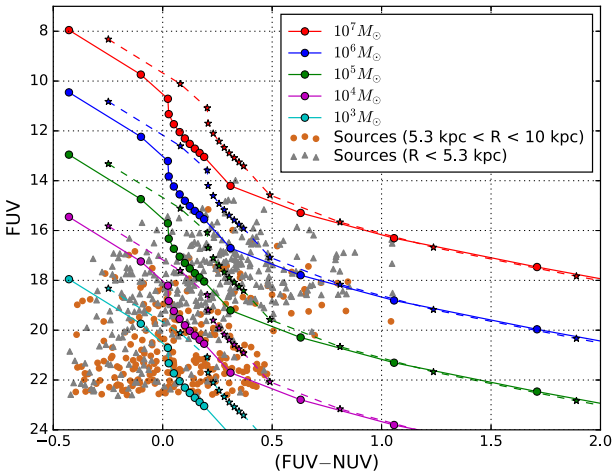

Figure 14. The selected UV sources are shown on the simulated plot presented in Figure 5. The sources present in the outer disk between radii 5.3 kpc to 10 kpc are shown in brown circles whereas gray diamonds represent the sources in the inner disk within radius 5.3 kpc.

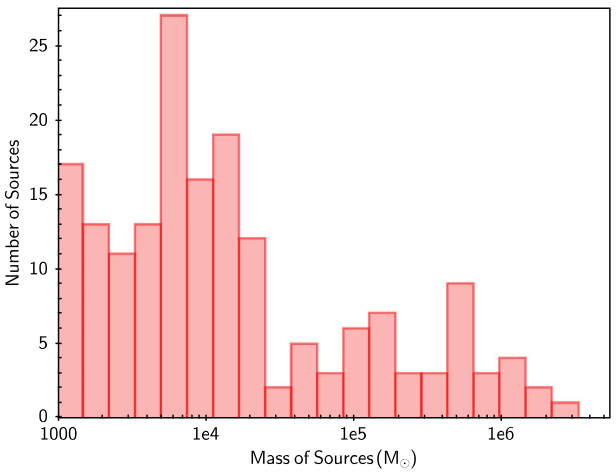

Figure 15. Mass histogram of the detected UV sources present between radius 5.3 kpc and 10 kpc. Sources with mass below $10^3 M_\odot$ are not displayed in the figure.

of NGC 300 and to understand the age and mass distribution of UV sources in the outer disk of the galaxy.

The detection of several extended structures in the FUV image strongly validates the presence of an outer disk in NGC 300. The galaxy is found to form substantially large number of objects during the last 25 Myr in its outer disk. The spiral arm present in the north-eastern direction is mainly populated by these young sources. Though we see a low level optical emission from this region of the galaxy, the detection of a significant number of young sources in the UV image conveys that star formation in the north-eastern spiral arm is a recent phenomenon.

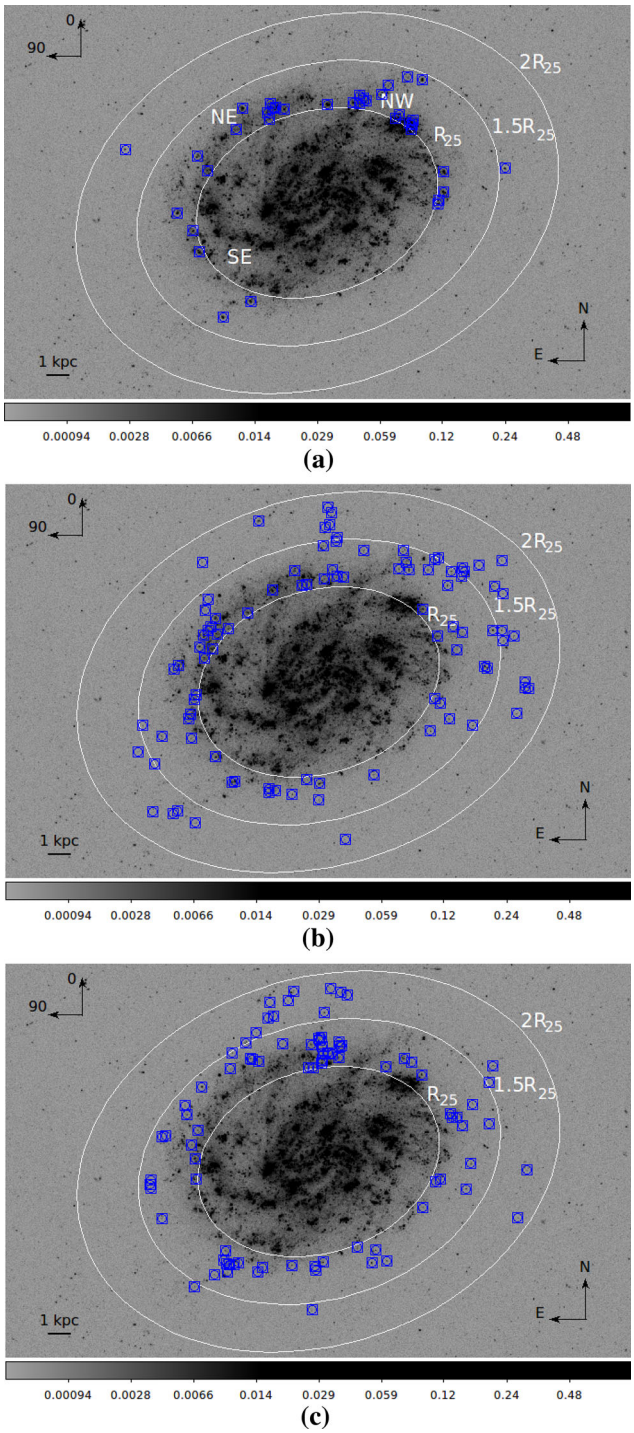

Figure 16. The mass distribution of the UV sources in the outer disk of the galaxy. **(a)** The high mass ($M > 10^5 M_\odot$) sources, **(b)** the intermediate mass ($10^3 M_\odot < M < 10^5 M_\odot$) sources and **(c)** the low mass sources ($M < 10^3 M_\odot$) are shown.

Rodríguez *et al.* (2016) identified 1147 young stellar groups by studying six different regions of NGC 300 through HST observations. They reported an age range from 1 to 235 Myr for all the stars present in the blue

bright groups. Using another HST observation, Hillis *et al.* (2016) identified 576 stars with an age between 10 to 200 Myr in one of their chosen fields. We have also obtained an age range of 1–300 Myr for the selected sources in our study.

The radial luminosity density profiles in different wavebands suggest that the disk of NGC 300 gradually becomes more steeper from shorter to longer wavelength. The scale-length estimated in FUV is found to be 2.3 times larger than that in the infrared. This signifies that the older populations are more centrally concentrated in the galaxy disk whereas the younger ones show more extended distribution. This also confirms the presence of XUV disk in NGC 300. The radial profile of the H I column density show a relatively flatter profile which suggests that star formation can trigger in the outer disk of the galaxy under favourable conditions.

Another important finding is the correlation between the H I map and the identified young UV sources. The north-eastern spiral arm, prominently seen in the UV image, is found to coincide with the dense H I gas. A large fraction of the young sources are also identified along this arm. The galaxy is believed to move in the south-east direction (Westmeier *et al.* 2011), which has caused the compression of H I gas in the south-east part of the disk. The H I contour map also shows a compression in the north-eastern direction, followed by dense H I gas. The star formation in the north-east region is likely to be due to this compression. We also detect a clump of low mass sources at the base of the northern extended structure.

With the help of Starburst99 SSP model, we have analysed the GALEX photometric data of the galaxy, NGC 300, and estimated the age and mass of identified sources present in the outer disk. As these sources are likely to be star clusters, we derive the recent cluster formation history of the galaxy. As the formation of clusters is closely related to the formation of stars in general, the cluster formation episodes are likely to suggest star formation episodes as well.

The parameters estimated in this study are based on the SSP model. We have assumed instantaneous star formation and stellar IMF as Kroupa, which is appropriate to study star formation in nearby galaxies. The errors of the estimated parameters (age and mass) are calculated from the photometric errors of both FUV and NUV magnitudes. The range of photometric error for the (FUV–NUV) color is 0.01–0.10. This error will reflect in the estimated age of the sources. The error in age for most of the sources present in the outer disk is less than 20 Myr. Some of the young sources (age < 150 Myr) show larger error whereas sources older than 200 Myr have less error in the estimated age. The photometric error in the FUV magnitude will contribute to the error in the estimation of the mass. This error also has a range 0.01–0.10, which corresponds to 0.5–5% error in the estimated mass for all the sources. The estimation of age has a dependency on reddening and metallicity. We have assumed moderate reddening and any decreased reddening will make the ages younger. The metallicity for the entire disk is assumed to be solar. If there is a significant gradient in the metallicity, the age estimation will be affected by the dependency as can be seen in Figure 4. The estimation of mass also has a dependence on the adopted extinction correction. As our study primarily explores the recent star- forming regions, we have assumed a moderate value of reddening and thus extinction. Any reduction in the assumed reddening will increase the FUV magnitude and the mass of a source and vice versa.

The outer disk of NGC 300 shows low level UV luminosity whereas optical studies indicate the presence of an unbroken stellar disk (Bland-Hawthorn *et al.* 2005). We detected several low mass sources in the outer disk of the galaxy. We found that the wispy extension of inner disk identified by Thilker *et al.* (2007) is due to these low mass young sources and slightly older intermediate mass sources. The low level star formation in the outer disk of NGC 300 may happen because of the less-availability of H I. Mild perturbation due to the motion of the galaxy and RAM pressure of the sculptor group medium could be causing the star formation in the outer disk. Therefore, this may be the process with which the outer disk is built in this galaxy.

The mass distribution of the selected UV sources suggests that the outer disk has predominantly formed low and intermediate mass sources ($M < 10^5 M_\odot$). Majority of young sources (age < 25 Myr) detected along the north-eastern spiral arm are found to have a low mass which signifies a low level recent star formation in the galaxy. We considered Kroupa IMF to estimate the mass of the UV sources with the help of the SSP model. Keeping other parameters the same (Table 2), we changed the IMF value to 2.35 (classical value, Salpeter 1955) with a stellar mass range from 0.1–120$M_\odot$ and estimated the mass of the sources. The estimated masses were 1.3–1.8 times the mass estimated using Kroupa IMF. The regions with intense 24 μm infrared emission in the galaxy spatially correlate with the massive star-forming complexes detected in the inner disk of NGC 300. Faesi *et al.* (2014) studied 76 H II regions in the disk of NGC 300 and estimated the stellar mass associated with each region. They found a range of mass from $10^3 M_\odot$ to $4 \times 10^4 M_\odot$. The young stellar

groups, identified by Rodríguez *et al.* (2016), with substantially large number of stars are also likely to have a total mass greater than $10^3 M_\odot$. In our study, we obtained a mass range from $10^3 M_\odot$ to $10^6 M_\odot$ (with some below $10^3 M_\odot$) for the sources present in the outer disk between 5.3 kpc and 10 kpc.

The nature of FUV luminosity density profile of NGC 300 points to the presence of an inner disk up to 5.5 kpc and an extended outer disk of at least up to 12 kpc. The SFR of NGC 300 is found to be $\sim$0.46 $M_\odot$/yr. Considering the GALEX FUV data, Verley *et al.* (2009) reported a SFR of $0.55 M_\odot$/yr for the galaxy M33. M33 is considered as the near optical twin of NGC 300 and they both have similar H I mass. Therefore, the comparable values of SFR observed in both the galaxies signifies that they are undergoing a similar state of star formation.

8. Summary

The main results of this study are summarized below:

1. Using GALEX UV data, we identified several extended structures in the outer part of the galaxy and confirmed the presence of an XUV disk in NGC 300.
2. The inner disk of the galaxy has a radius of 5.5 kpc whereas we detected an outer disk of at least up to radius 12 kpc.
3. The disk scale-length, which is found to increase gradually from longer to shorter wavelength, is estimated to be 2.66 ± 0.20 kpc in NUV and 3.05 ± 0.27 kpc in FUV.
4. We identified 261 candidate UV sources in the outer disk between radius 5.3 kpc to 10 kpc ($1 \sim 2R_{25}$) and estimated their age and mass by applying the SSP models.
5. We noticed a richness of younger (age < 25 Myr) as well as low and intermediate mass ($M < 10^5 M_\odot$) sources in the outer disk of the galaxy.
6. The star formation in the north-eastern spiral arm of the galaxy is a recent phenomenon, consisting of low mass sources with age < 25 Myr.
7. The distribution of the UV sources identified in the outer disk correlates well with the features of the H I density map.
8. Presently, the galaxy is undergoing a low level recent star formation in the outer disk ($\geq R_{25}$), which may be due to its motion in the Sculptor group.
9. The SFR of NGC 300 ($\sim$0.46 $M_\odot$/yr) is found to be comparable with its near optical twin M33.

Acknowledgements

This study has primarily used ultra-violet data from GALEX observation. We thank both the GALEX and MAST team for providing science ready data products to the public. This research has also made use of the NASA/IPAC Extragalactic Database (NED), which is operated by the Jet Propulsion Laboratory, California Institute of Technology, under contract with the National Aeronautics and Space Administration. This research made use of Matplotlib (Hunter 2007), community-developed core Python package. Finally, we thank the referee for valuable suggestions.

References

Azzollini R., Trujillo I., Beckman J. E. 2008, ApJ, 684, 1026
Barker M. K., Ferguson A. M. N., Cole A. A. *et al.* 2011, MNRAS, 410, 504
Barnes K. L., van Zee L., Skillman E. D. 2011, ApJ, 743, 137
Binder B., Williams B. F., Eracleous M. *et al.* 2012, ApJ, 758, 15
Bland-Hawthorn J., Vlajić M., Freeman K. C., Draine B. T. 2005, ApJ, 629, 239
Carignan C. 1985, ApJS, 58, 107
de Vaucouleurs G., de Vaucouleurs A., Corwin Jr. H. G. *et al.* 1991, S&T, 82, 621
de Vaucouleurs G., Page J. 1962, ApJ, 136, 107
Dong H., Calzetti D., Regan M. *et al.* 2008, AJ, 136, 479
Faesi C. M., Lada C. J., Forbrich J., Menten K. M., Bouy H. 2014, ApJ, 789, 81
Ferguson A., Irwin M., Chapman S. *et al.* 2007, Astrophys. Space Sci. Proc., 3, 239
Gazak J. Z., Kudritzki R., Evans C. *et al.* 2015, ApJ, 805, 182
Gil de Paz A., Madore B. F., Boissier S. *et al.* 2005, ApJL, 627, L29
Goddard Q. E., Kennicutt R. C., Ryan-Weber E. V. 2010, MNRAS, 405, 2791
Gogarten S. M., Dalcanton J. J., Williams B. F. *et al.* 2010, ApJ, 712, 858
Helou G., Roussel H., Appleton P. *et al.* 2004, ApJS, 154, 253
Hillis T. J., Williams B. F., Dolphin A. E., Dalcanton J. J., Skillman E. D. 2016, ArXiv e-prints, arXiv:1609.02106
Hunter J. D. 2007, Computing in Science & Engineering, 9, 90
Jerjen H., Freeman K. C., Binggeli B. 1998, AJ, 116, 2873
Karachentsev I. D., Kaisina E. I. 2013a, AJ, 146, 46

Karachentsev I. D., Grebel E. K., Sharina M. E. *et al.* 2003, A&A, 404, 93
Kennicutt R. C., Evans N. J. 2012, ARA&A, 50, 531
Kennicutt Jr. R. C. 1998, ApJ, 498, 541
Kim S. C., Sung H., Park H. S., Sung E.-C. 2004, ChJA&A, 4, 299
Knapen J. H., Mazzuca L. M., Böker T. *et al.* 2006, A&A, 448, 489
Kroupa P. 2001, MNRAS, 322, 231
Kudritzki R.-P., Urbaneja M. A., Bresolin F. *et al.* 2008, ApJ, 681, 269
Leitherer C., Schaerer D., Goldader J. D. *et al.* 1999, ApJS, 123, 3
Mondal C., Subramaniam A., George K. 2018, AJ, 156, 109
Morrissey P., Conrow T., Barlow T. A. *et al.* 2007, ApJS, 173, 682
Puche D., Carignan C., Bosma A. 1990, AJ, 100, 1468
Rizzi L., Bresolin F., Kudritzki R.-P., Gieren W., Pietrzyński G. 2006, ApJ, 638, 766
Rodríguez M. J., Baume G., Feinstein C. 2016, A&A, 594, A34
Salpeter E. E. 1955, ApJ, 121, 161
Skrutskie M. F., Cutri R. M., Stiening R. *et al.* 2006, AJ, 131, 1163
Thilker D. A., Bianchi L., Boissier S. *et al.* 2005a, ApJL, 619, L79
Thilker D. A., Bianchi L., Meurer G. *et al.* 2005b, in: Bulletin of the American Astronomical Society, Vol. 37, American Astronomical Society Meeting Abstracts, 1500
Thilker D. A., Bianchi L., Meurer G. *et al.* 2007, ApJS, 173, 538
Tully R. B., Rizzi L., Dolphin A. E. *et al.* 2006, AJ, 132, 729
Verley S., Corbelli E., Giovanardi C., Hunt L. K. 2009, A&A, 493, 453 15
Vlajić M., Bland-Hawthorn J., Freeman K. C. 2009, ApJ, 697, 361
Westmeier T., Braun R., Koribalski B. S. 2011, MNRAS, 410, 2217
Wilsey N., Hunter D. 2010, in: Bulletin of the American Astronomical Society, Vol. 42, American Astronomical Society Meeting Abstracts 215, 481
Xu C. K., Donas J., Arnouts S. *et al.* 2005, ApJL, 619, L11
Yuan H. B., Liu X. W., Xiang M. S. 2013, MNRAS, 430, 2188
Zaritsky D., Christlein D. 2007, AJ, 134, 135